

CALCULATION OF LONGITUDINAL INSTABILITY THRESHOLD CURRENTS FOR SINGLE BUNCHES *

P. Kuske, Helmholtz-Zentrum Berlin für Materialien und Energie, Germany

Abstract

Based on the publication by M. Venturini, et al. [1] a computer program has been developed that solves the Vlasov-Fokker-Planck equation numerically on a two dimensional grid. In this code different types of longitudinal interactions and their combinations are implemented. Calculations have been performed for the 1.7 GeV storage ring BESSY II and the 600 MeV ring MLS using the wake created by the shielded coherent synchrotron radiation (CSR). The results are compared with measurements on both rings which were based on the observation of the onset of time dependent fluctuations ("bursts") of CSR [2, 3]. Fair agreement is found between theory and experiment. The theoretical results complement calculations performed by Bane, et al. [4] for this type of interaction. The new results emphasize the resistive nature of the CSR-interaction, especially in regions where shielding effects are small or the resonance-like features of this wake are important. It is found that in these regions the instability is weak and thresholds depend on the damping time.

INTRODUCTION

The longitudinal stability of a single bunch of charged particles circulating in a storage ring is still a domain of active experimental and theoretical research. On the experimental side the observation of CSR has supplemented the conventional RF-techniques and extended the region of observation frequencies into the THz part of the bunch spectrum. Thus the time resolution reaches the fs-region. Already the first observations of the time dependent CSR at BESSY II created the desire to compare theoretical and experimental results [2]. On the theoretical side the most advanced semi-analytical approach has been introduced by Oide and Yokoya [5], however, predictions based on their approach are ambiguous. Multi particle tracking codes suffer from the rather high shot noise and therefore a numerical solution of the Vlasov-Fokker-Planck (VFP) equation was chosen for the theoretical modelling [2,6].

THEORETICAL MODEL

The ensemble of electrons is described by a distribution function, $\psi(q,p,\tau)$, which can be written in terms of the normalized phase-space coordinates: $q=z/\sigma_z$, $p=(E_0-E)/\sigma_E$, and τ , in units of the synchrotron period, $1/\omega_s$. The low current rms bunch length, σ_z , and the natural energy spread, σ_E , are related by: $\omega_s\sigma_z/c=\alpha\sigma_E/E_0$ with c , the speed of light, and α , the momentum compaction factor. The VFP equation describes the evolution of the

distribution which depends on the radiation excitation and damping and the interaction of the particles [1]:

$$\frac{\partial\psi}{\partial\tau} + p\frac{\partial\psi}{\partial q} - [q + F_c(q,\tau,\psi)]\frac{\partial\psi}{\partial p} = \frac{2}{\omega_s t_d} \frac{\partial}{\partial p} \left(p\psi + \frac{\partial\psi}{\partial p} \right)$$

The r.h.s. is the Fokker-Planck-term which introduces damping and diffusion and t_d is the longitudinal damping time. The coefficient in the square brackets is the approximated linear restoring force of the RF-potential and F_c is the collective force from the interaction of the charge distribution with itself and its metallic surrounding. This force or the induced voltage is obtained by the convolution of the longitudinal charge density with the wake function. The charge density, $\lambda(q,\tau)$, is given by $\lambda(q,\tau)=\int dp \psi(q,p,\tau)$. The wake function depends on the types of interactions studied.

Numerical Solution of the VFP-Equation

Warnock, et al [7] and Venturini, et al [1] proposed two different numerical algorithms to find the distribution function on a two dimensional grid as a function of time. In both cases the required extrapolation of the distribution function to off-grid points can lead to unrealistic negative values for $\psi(q,p,\tau)$. Therefore, a kind of wave function, $g(q,p,\tau)$, is introduced so that the probability to find electrons is given by $\psi(q,p,\tau)=g^2(q,p,\tau)$ and always larger than zero. As a result only the Fokker-Planck-term needs to be modified in the VFP equation for $g(q,p,\tau)$:

$$\frac{\partial g}{\partial\tau} + p\frac{\partial g}{\partial q} - [q + F_c] \frac{\partial g}{\partial p} = \frac{2}{\omega_s \tau_l} \left(\frac{g}{2} + p\frac{\partial g}{\partial p} + \frac{1}{g} \left(\frac{\partial g}{\partial p} \right)^2 + \frac{\partial^2 g}{\partial p^2} \right)$$

This equation is solved by splitting the time step, $\Delta\tau$, of the temporal evolution of the wave function, $g(q,p,\tau)$, into smaller steps [1]:

$$\begin{aligned} g_1(q,p,\tau) &= g_0(q-p\cdot\Delta\tau/2,p,\tau) \\ g_2(q,p,\tau) &= g_1(q,p+(q+F_c(q,g_0))\cdot\Delta\tau,\tau) \\ g_3(q,p,\tau) &= g_2(q-p\cdot\Delta\tau/2,p,\tau) \\ g_4(q,p,\tau+\Delta\tau) &= g_3(q,p,\tau) + \text{diffusion} + \text{damping} \end{aligned}$$

The code uses a fourth order polynomial in order to interpolate to off-grid points. The interpolation is performed between the grid points $g(x-2\Delta)$, $g(x-\Delta)$, $g(x)$, $g(x+\Delta)$ and $g(x+2\Delta)$ and thus is more symmetric relative to the central point compared to a cubic Hermite interpolation [1]. x stands for the p or q coordinate and Δ is the distance between grid points. The first step coded in BASIC looks like this:

```
For iq = -iqmax To iqmax: For ip = -ipmax To ipmax
  g0 = gold(iq, ip)
  If Abs(g0) > .000001 Then
    dQ = - ip *deltaP/deltaQ* dtau / 2
    gmm = gold(iq - 2, ip): gm = gold(iq - 1, ip)
```

*Work supported by the BMBF and the Land Berlin

```

gp = gold(iq + 1, ip): gpp = gold(iq + 2, ip)
a1=(gmm-8*gm+8*gp-gpp) / 12*dQ
a2=(-gmm+16*gm-30*g0+16*gp-gpp)/24*dQ^2
a3=(-gmm+2*gm-2*gp+gpp)/12*dQ^3
a4=(gmm-4*gm+6*g0-4*gp+gpp)/24*dQ^4
gnew(iq, ip) = (g0 + a1 + a2 + a3 + a4)
End If

```

Next ip: Next iq

The second step looks very similar. In all steps terms are only included for sufficiently large values of g , i.e. $|g| > 10^{-6}$. The final diffusion and damping step is coded in the following way:

For iq = -iqmax To iqmax: For ip = -ipmax To ipmax

```
g0 = gold(iq, ip)
```

```
If Abs(g0) > .000001 Then
```

```
gp = gold(iq, ip + 1): gm = gold(iq, ip - 1)
```

```
g1 = (4*gp-6*g0+4*gm-2*gp*gm/g0)/deltaP ^ 2
```

```
g1=g1+ ip*(gp-gm) + (g0+gp)/2
```

```
gnew(iq, ip)= g0+g1*beta*dtau
```

```
End If
```

Next ip: Next iq

Just a few lines of code are required in order to follow the temporal evolution of the distribution function. The calculation could be speeded up by storing and updating the two partial derivatives, $\partial g/\partial q$ and $\partial g/\partial p$, of the amplitude function. This is not done since the mesh size can become quite large [6] for certain calculations. For the stability studies presented here usually a 256 by 256 mesh ($ipmax=qmax=128$) with a spacing of $\sigma/10$ is used. Stability of the algorithm requires a certain number of steps per synchrotron period in proportion to the damping and excitation given by $\omega_s \tau_1 = 1/\beta$. For the cases studied here 512 to 1024 steps with $\Delta\tau = 2\pi/512$ or $\Delta\tau = 2\pi/1024$ are sufficient. The temporal evolution of the particle distribution is followed over as many synchrotron periods as required to cover at least 6 and up to 10 damping times. This can be thousands of periods. If the resolution is increased also the number of steps must go up. Doubling the resolution leads to an 8-fold increase in the computing time. Instability thresholds and features of the instability do not change significantly if the resolution is increased.

RESULTS

In Table 1 the relevant parameters for the longitudinal single bunch dynamics of the two storage rings are collected. The simulations begin with the potential well distorted distribution function which implies that the beam is longitudinally stable and has a Gaussian energy distribution with a normalised rms width, σ_E , equal to 1. In the threshold calculations the current is increased or decreased by small amounts and simulations continue with the previously found distribution. If approached from below the current threshold is reached as soon as $\sigma_E > 1$. The code was compared successfully to the weak instability created by a resistive δ -function wake, $w(q) = R\delta(q)$ [8]. The results of this simulation showed more strongly increasing threshold currents as $\omega_s \tau_1 / 2\pi$ approaches 1. On the other hand, simulations with an

inductive wake, $w(q) = L \cdot T_0 / 2\pi \partial \delta(q) / \partial q$, as expected showed no instability at all. In addition, results using the wake of a broad band resonator (BBR) have been compared to predictions of other calculations [4]. The present detailed simulation reproduces these results and certain jump-like changes in parameters like the frequency of the first unstable mode similar to what can be observed in experiments [9] and where the semi-analytical approach [5] fails.

Table 1: Parameters Used in the Simulations

Parameter	BESSY II	MLS
Energy, E_0/MeV	1700	629
Bending radius, ρ/m	4.35	1.528
Momentum compaction, α	$7.3 \cdot 10^{-4}$	$1.3 \cdot 10^{-4}$
Cavity voltage, V_{rf}/kV	1400	330
Accelerating frequency, ω_{rf}/MHz	$2\pi \cdot 500$	$2\pi \cdot 500$
Revolution time, T_0/ns	800	160
Natural energy spread, σ_E	$7.0 \cdot 10^{-4}$	$4.36 \cdot 10^{-4}$
Zero current bunch length, σ_0/ps	10.53	1.549
Longitudinal damping time, τ_l/ms	8.0	11.1
Synchrotron frequency, ω_s/kHz	$2\pi \cdot 7.7$	$2\pi \cdot 5.82$
Height of the dipole chamber, $2h/\text{cm}$	3.5	4.2

The impact of the CSR-wake with parallel plate shielding [6] has been simulated for both rings. The threshold currents are displayed in Figure 1 together with some experimental results and using a scaling introduced by Ries, et al. [3]. At the MLS and for bunches longer than 1 mm the findings in this publication agree quite well with the theoretical predictions. For bunches shorter than 2 mm the simulated thresholds depend strongly on the synchrotron tune in relation to the damping time. This characterises the weak instability mechanism. The simulation for $V_{rf} = 500$ kV and for 1 - 2 mm long bunches (not shown for clarity) would overlap the curve for BESSY II. At higher cavity voltages and with shorter bunches the predictions are approaching the results of

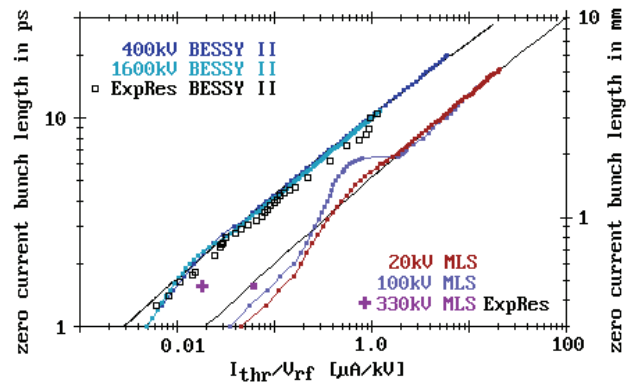


Figure 1: Comparison of theoretical (colour lines) and experimental results for the CSR-instability threshold currents. The black solid line is the theoretical curve from Bane, et al. [4]. They already predicted a deviation from that line around a certain bunch length. Clearly visible in the MLS results and much less pronounced for BESSY II.

Bane, et al. [4]. In Figure 1 only one of the experimental results of the MLS is included: the case with a cavity voltage, V_{rf} of 330 kV and a momentum compaction factor of $\alpha=1.3 \cdot 10^{-4}$. In general, for the shorter bunches the observations at the MLS and simulations disagree.

Similar measurements performed at BESSY II do agree much better with the general trend of the theory [4]. A typical result of a CSR measurement at BESSY II for a short bunch can be seen in Figure 2. The instability sets in at around 11.5 μ A with a fast growing line between the 3rd and 4th harmonic of the synchrotron frequency. For these short bunches, where the impact of the shielding is small, the CSR distorted bunch shape is very similar to the distortion created by a resistive wake. With such a wake and with $1/\omega_s\tau_1$ approaching 1 the threshold currents are shifted to higher values in agreement with expectations [8] for a weak instability. This happens in both rings, however, could not yet be verified experimentally. At the MLS the transition to a strong instability occurs at higher cavity voltages (i.e. 330 kV).

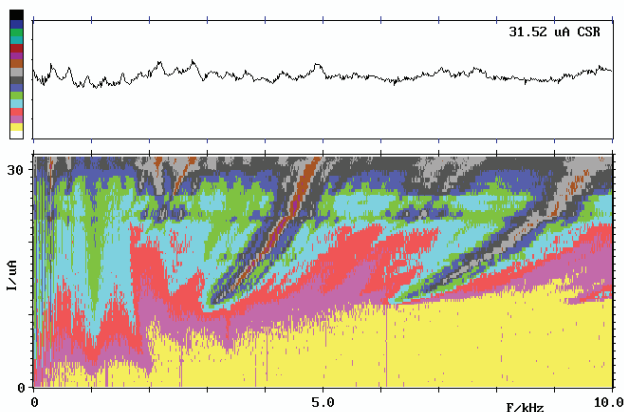


Figure 2: FFT spectra of the temporal THz-signals recorded as a function of increasing current showing remarkable features of the synchrotron sidebands. The zero current synchrotron frequency is 1 kHz and the rms bunch length is ~ 1.4 ps. The logarithmic plot of the spectrum at 31.5 μ A is shown in the top and the colours span 6 orders of magnitude.

Figure 3 shows a comparison of the frequency of the first unstable mode at BESSY II. The slope of the experimental [9] and the theoretical data agree quite well. The slope depends on the bunch length and the peak frequency of the resonator-like CSR-impedance, given by $F_{res}/c=(\pi\rho/24h^3)^{1/2}$ [10]. Significant deviations are found for the shortest bunches. There the shielding is less important and one would expect that the $m=2$, quadrupole mode, has the lowest threshold [8], it is rather the $m=3...4$ mode which becomes unstable first, see Figure 2.

SUMMARY

In conclusion, calculations with a shielded CSR-wake are generally in surprisingly good agreement with the measurements. This wake alone does not reproduce some

of the observed features of the longitudinal single bunch dynamics like the strong "inductive" lengthening or the "resistive" shift and shape distortion observed with the streak camera [11]. However, the observations on two different storage rings in accord with the simulations demonstrate the importance of the shielded CSR-wake and thus the dipole chamber geometry: the slope of the first unstable mode frequency observed at BESSY II in agreement with a broad band resonator with $F_{res}\sim 100$ GHz and the pronounced threshold behaviour at the MLS with a bunch length around 2 mm with $F_{res}\sim 44$ GHz. Simulations with a more realistic model of the vacuum chamber and a more elaborate CSR-wake [12] should improve the agreement with the observations. The final goal still is the theoretical modelling of measured spectra similar to Figure 2, and which are usually much more complex at higher intensities.

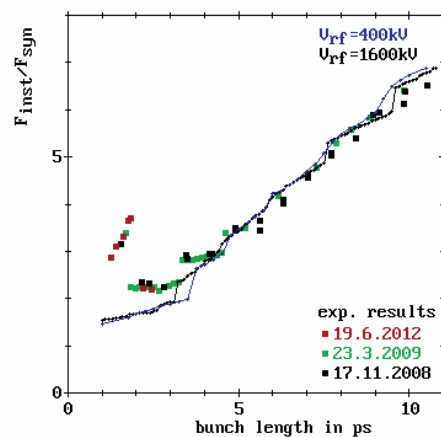


Figure 3: Frequency of the first unstable mode in units of the synchrotron frequency as a function of the zero current bunch length. The simulation was performed for two different cavity voltages and, like in the experiment with $V_{rf}=1.4$ MV, the momentum compaction factor was varied in order to change the length of the bunches.

ACKNOWLEDGMENT

The support of K. Holldack with the THz-detector is acknowledged. G. Wüstefeld is thanked for making the experimental results of the MLS available prior to publication.

REFERENCES

- [1] M. Venturini, et al., Phys. Rev. ST-AB **8**, 014202 (2005)
- [2] M. Abo-Bakr, et al., PAC'03, RPPB006, www.JACoW.org
- [3] M. Ries, et al., IPAC'12, WEPPR046, www.JACoW.org
- [4] K.L. Bane, et al., Phys. Rev. ST-AB **13**, 104402 (2010)
- [5] K. Oide and K. Yokoya, KEK-Preprint-90-10, April 1990
- [6] P. Kuske, IPAC'11, THPO025, http://www.JACoW.org
- [7] R. Warnock and J.A. Ellison, SLAC-PUB-8404 (2000)
- [8] K. Oide, Part. Accel. **51**, 43 (1995)
- [9] P. Kuske, PAC'09, FR5RFP063, www.JACoW.org
- [10] R.L. Warnock, PAC'91, PAC1991_1824, http://www.JACoW.org
- [11] M. Abo-Bakr, et al., PAC'93, RPPB005, www.JACoW.org
- [12] D. Zhou, et al., IPAC'11, WEPC108, www.JACoW.org